Foundation University Journal of Engineering and Applied Sciences

FUJEAS
Vol. 5, Issue 1, 2024
DOI: 10.33897/fujeas.v5i1.744

Research Article

Discerning of Hall Effect in Technology using New Data Acquisition Technique

Anum Zaidi [a], Amad Ud Din [a, *], Hammad Ul Hassan [b], Muhammad Sahil [b], Fasih Ud Din [c], Muhammad Kamran [d]

[a] Department of Physics, Fatima Jinnah Women University, Rawalpindi, Rawalpindi, Pakistan.
[b] Department of Physics, Air University, Islamabad, Pakistan.
[c] Department of Physics, Grand Asian University, Sialkot, Rawalpindi, Pakistan.
[d] Department of Electrical Engineering, COMSATS University, Wah-Cantt. Campus, Wah Cantt., Pakistan.

* **Corresponding author**: dr.amad1947@gmail.com

Abstract:

Certain areas of physics are revolutionized by modern technology, and the Hall Effect Apparatus (HEA) is one of those, as this apparatus has a lot of importance. To study the HE apparatus, an electronics-based system is designed through which one can be informed about the Hall Voltage (V_H), Hall Coefficient (R_H), and the type of majority charge carriers in semiconductor samples using microcontrollers with a built-in graphic user interface (GUI) as a stand-alone system. The purpose is to develop and upgrade the HE apparatus using advanced data acquisition techniques and introduce microcontrollers for a GUI to obtain electronic data and graphical representations. The measured results show that the system can produce 90% results at 10 times lower cost. Generally, three semiconductor samples were taken to observe the Hall Effect parameters using the HE Apparatus, and remarkable relative results with the literature were observed. Carrier concentration for *CdHgTe*, *ZnO,* and Silicon were $-10\times10^{20}/cm^3$, $-2\times10^{18}/cm^3$, and $7.5\times10^{18}/cm^3$, respectively, using the I/V slope from the plots obtained at different magnetic fields. Similarly, the Hall coefficients, Hall Mobility, and the Resistivity.

Keywords: Semiconductor Material; Hall Effect; Hall Voltage; Hall Coefficient and Charge Carrier Concentration.

Article Citation:
Zaidi et al. (2024). "Discerning of Hall Effect in Technology using New Data Acquisition Technique". *Foundation University Journal of Engineering and Applied Sciences*
DOI:10.33897/fujeas.v5i1.744

Published by
Foundation University
Islamabad.
Web: https://fui.edu.pk/

1. Introduction

In this mechanized age, technology is an integral part of everyday life, driving advancements across various fields, including physics. It is defined as the combination of techniques, skills, methods, and processes used to produce goods or achieve specific goals, such as scientific investigations. Technology has significantly increased the efficiency of our work, allowing us to employ sophisticated tools and methods that accelerate the pace of innovation, thus having a profound impact on human life [1].

One notable technological advancement in physics is the development of the Hall Effect Apparatus (HEA). This apparatus is instrumental in investigating the Hall Effect, a phenomenon discovered by Edwin Herbert Hall in 1879, which reveals the deflection of charge carriers, like electrons, by a magnetic field [2]. This effect is characterized by the ratio of the induced electric field to the product of the current density and the applied magnetic field, serving as a fundamental property of materials that depends on the type, number, and properties of charge carriers [3]. The

Hall Effect is crucial in understanding the electrical properties of materials, particularly semiconductors, and has applications in developing electronic devices and sensors [4].

The Hall Effect Apparatus has evolved with modern technology to incorporate advanced data acquisition techniques and graphical interfaces. These improvements have enhanced the precision and accessibility of experiments, enabling researchers and educators to determine critical parameters such as Hall Voltage (V_H), Hall Coefficient (R_H), and the type of majority charge carriers in semiconductor samples [5-6]. The use of microcontrollers with built-in graphical user interfaces (GUIs) has transformed the HEA into a user-friendly platform for analyzing and visualizing data, expanding the scope of experimentation in both educational and research environments [7-8]. The modernization of the HEA has allowed for the study of a variety of semiconductor materials, such as cadmium mercury telluride (*CdHgTe*), zinc oxide (*ZnO*), and silicon. These materials exhibit unique electrical properties, making them ideal for examining the impact of the Hall Effect on carrier concentration, mobility, and resistivity [9][10]. Understanding these parameters is essential for developing new electronic devices and enhancing the field of semiconductor physics [11], [12].

This paper introduces a cost-effective and technologically advanced Hall Effect Apparatus (HEA) that enhances applied physics research. By incorporating modern microcontroller technology and a graphical user interface (GUI), the new HEA system provides precise data acquisition and visualization at a significantly lower cost than traditional systems. This innovation improves accessibility for educational and research institutions and offers accurate measurements of V_H, R_H, and charge carrier properties in materials such as CdHgTe, ZnO, and silicon.

2. Related Work

The study of the Hall Effect and its applications has been a focal point of research in condensed matter physics. Several studies have explored the capabilities of the Hall Effect Apparatus in measuring the electrical properties of semiconductors. Borsos et al. [5] investigated new data acquisition and processing methods for the Hall Effect experiment, demonstrating improved accuracy and efficiency in determining material properties. Their work highlighted the potential for modernizing the HEA to enhance experimental outcomes. The research conducted by Sconza and Torzo [8] provided insights into measuring the energy gap in semiconductors using undergraduate laboratory experiments. This study emphasized the educational value of the HEA in fostering a deeper understanding of semiconductor physics among students. The integration of advanced technologies in these experiments has improved the precision and reliability of the results, making the HEA an indispensable tool in academic settings.

In recent years, efforts have been made to expand the application of the Hall Effect Apparatus to a broader range of materials. For instance, the work by Thompson et al. [10] focused on the growth of CdHgTe by metal-organic chemical vapor deposition (MOCVD) and its implications for material properties. This study underscored the importance of the HEA in characterizing semiconductor materials and guiding the development of new electronic devices.

Further advancements in the field have explored the modification of semiconductor surfaces through techniques such as ion implantation and thermal annealing. Research by Korotaev et al. [12] examined the effects of these processes on HgCdTe, demonstrating the versatility of the HEA in studying surface modifications and their impact on material performance. This line of inquiry has significant implications for applications in optoelectronics and nanotechnology.

3. Hall Effect Parameters

3.1. Hall Coefficient

Through HE experiments, one can get the following main information about the samples that are being tested. This 1/qn is the Hall coefficient, and RH is equal to ($V_H \cdot$ W)/BI. In the same way for the P-type

materials, with the only difference being that holes are the majority charge carriers, i.e., RH = 1/qp = 1/qn, where q is charge. The symbols n and p are the electron and hole densities, respectively. The value of RH determines the type of semiconductors. The positive value of RH shows that the sample is p-type, and the negative value of RH shows that the sample is n-type [2].

3.2. Hall Voltage and Types of Semiconductors

The sign of Hall voltage (V_H) indicates the type of semiconductor. For a p-type semiconductor, V_H is positive, for an n-type semiconductor, V_H is negative, and for an intrinsic semiconductor, V_H is zero.

3.3. Carrier Concentration

Carrier concentration is one of the basic HE parameters to determine the other parameters for electrons, and its value can be determined using $\boldsymbol{n = -\frac{I_x B_z}{t_q} V_H}$. For n-type semiconductors, the value of $\boldsymbol{V_H}$ will be negative. Similarly, for p-type semiconductors, one can proceed in the same way to get the majority carrier concentration, and the net result will be similar except for a positive sign due to the positive charge. $\boldsymbol{V_H}$ that is using $\boldsymbol{p = +\frac{I_x B_z}{tq} V_H}$.

3.4. Mobility

The equation of mobility using the equation for charge density can be written as,

$$\mu_n = \frac{I_x L}{wtqnV_x} \quad (1)$$

and like all other parameters, we can do the same calculations for the mobility of the majority charge carrier in p-type semiconductors, which is given by:

$$\mu_p = \frac{I_x L}{wtqpV_x} \quad (2)$$

Where μ_p is the mobility of a hole, and it depends on the length, width, and depth of the semiconductor. All the apparatuses presently working all over the world are manual-based, and those who use some data acquisition techniques have a lot of off-board devices like computers, power supplies, etc. [3].

There are a few apparatuses presently working to measure Hall parameters, as follows:

Some apparatuses are used in the old-fashioned experimental setup in which data was obtained using analogue multi-meters, which have a lot of wiring and complex mechanisms.

Some proposed a complex experimental setup in which software and interfaces between the experimental setup and the computer were introduced. Also, separate PCs were allocated as a display unit.

A few setups introduced different experimental components, including a Hall probe, Gauss meter, electromagnets, and power supplies. They used a Gauss meter in combination with a Hall probe to estimate and measure the strength of the magnetic field.

In the following sections, a brief system overview and the complete instrumentation of the experimental setup are presented. Also, the working and results obtained by the devices will be discussed [4].

4. System Overview

This is a single unit having all measurements on the same board, and its block diagram is shown in Figure 1. This is an automated system which do not require a separate voltmeter, ammeter, and power supply to measure the Hall Effect (HE) parameters, as the system can collect the data automatically and display it through a graphical user interface. It is user-friendly, efficient, and cost-effective.

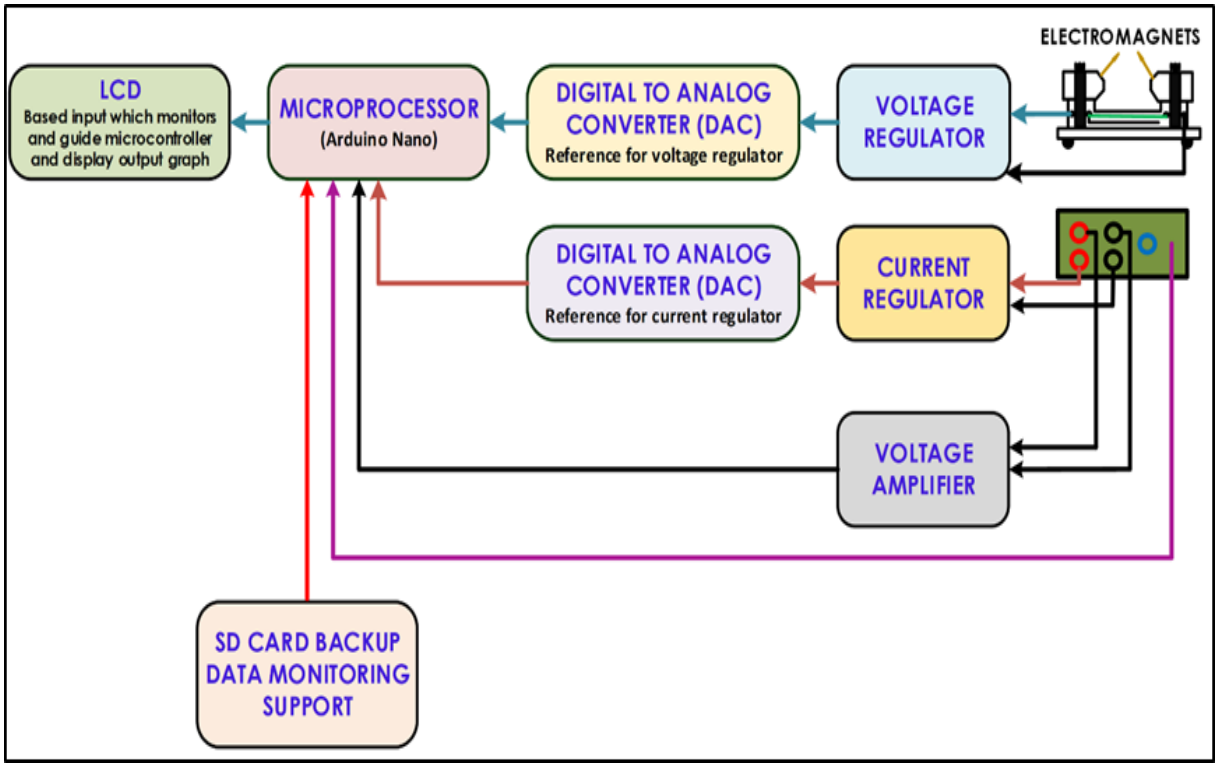

Figure 1: Block diagram of the system to measure Hall Effect parameters

Semiconductor materials mostly behave as insulators at room temperature. In this assembly, a temperature chamber is also introduced, which will help to study different hall parameters at different temperatures as well. The device will be helpful to determine the doping type, like n-type or p-type, in semiconductors like solar cells. The other parameters, like mobility, Hall coefficient (R_H), and Hall voltage (V_H), help to determine the carrier concentration in semiconductor materials. A flow diagram for the Hall Coefficient is shown in Figure 2 for better understanding [5].

The microprocessor collects information about the magnetic field of electromagnets through a Hall sensor attached to the sample printed circuit board. It also reads the applied sample current across the semiconductor sample in the range of mA, which was supplied through the current regulator circuit powered by a power supply. Then it records the hall voltage of the mV range across the semiconductor sample powered by the sample current and placed in a transverse magnetic field. The measured hall voltage is further useful to get the number of charge carriers and the type of charge carriers in semiconductors. Through coding, the device will be able to display recorded parameters directly to the LCD and will be able to plot a graphical representation automatically without any manual assistance [6], [7].

5. Device Components and Design

The components like electromagnets, power supply, Arduino Nano microcontroller, display unit, Hall sensor, regulators, Sample PCB, and heating chamber were used in the construction of the assembly, as shown in the Figure. 3. The complete assembly setup is controlled through the software. The details of these are as follows:

5.1. Electromagnet

It has 400 turns on each side of a U-shaped (Figure 4) electromagnet to produce a magnetic field of about 3000 Gauss, but we only need a magnetic field of about 1800 Gauss. The choice of 400 turns on each side of the electromagnet to produce a magnetic field of about 1800 Gauss is based on the

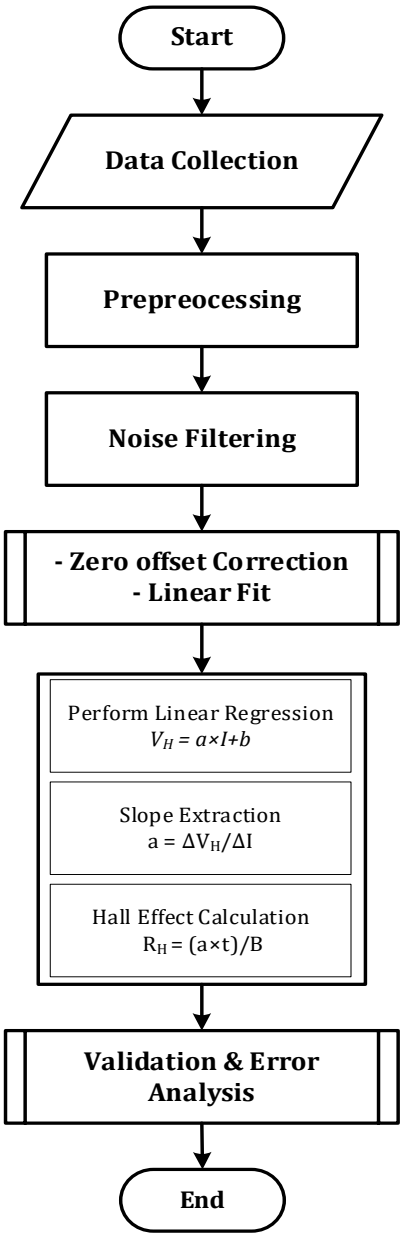

Figure 2: Flow diagram for the Hall coefficient

relationship between the number of turns, the current, and the magnetic field strength. The formula for the magnetic field B in a solenoid is: $B=\mu_0*(N*)/L$. By selecting 400 turns, the design ensures a sufficient magnetic field strength at a practical current level, optimizing both the magnetic field generation and power consumption.

The electromagnetic is connected to the variable power supply. Then a Gauss meter is used to measure the initial magnetic field strength. Gradually increased the current using the power supply while continuously measuring the magnetic field strength. In order to achieve 1800 Gauss, a smaller adjustment is made to the current for precise control. Then we allow the electromagnet to stabilize and recheck the field strength to ensure it consistently reads 1800 Gauss.

5.2. Power Supply

To supply power to different components that are used in assembly-like electromagnetic, Arduino board, display unit, sensors, and sample board, we used a linear power supply whose specifications include a power of 130.65 watts, an output voltage of 19.5 V, and a current of 6.7 A.

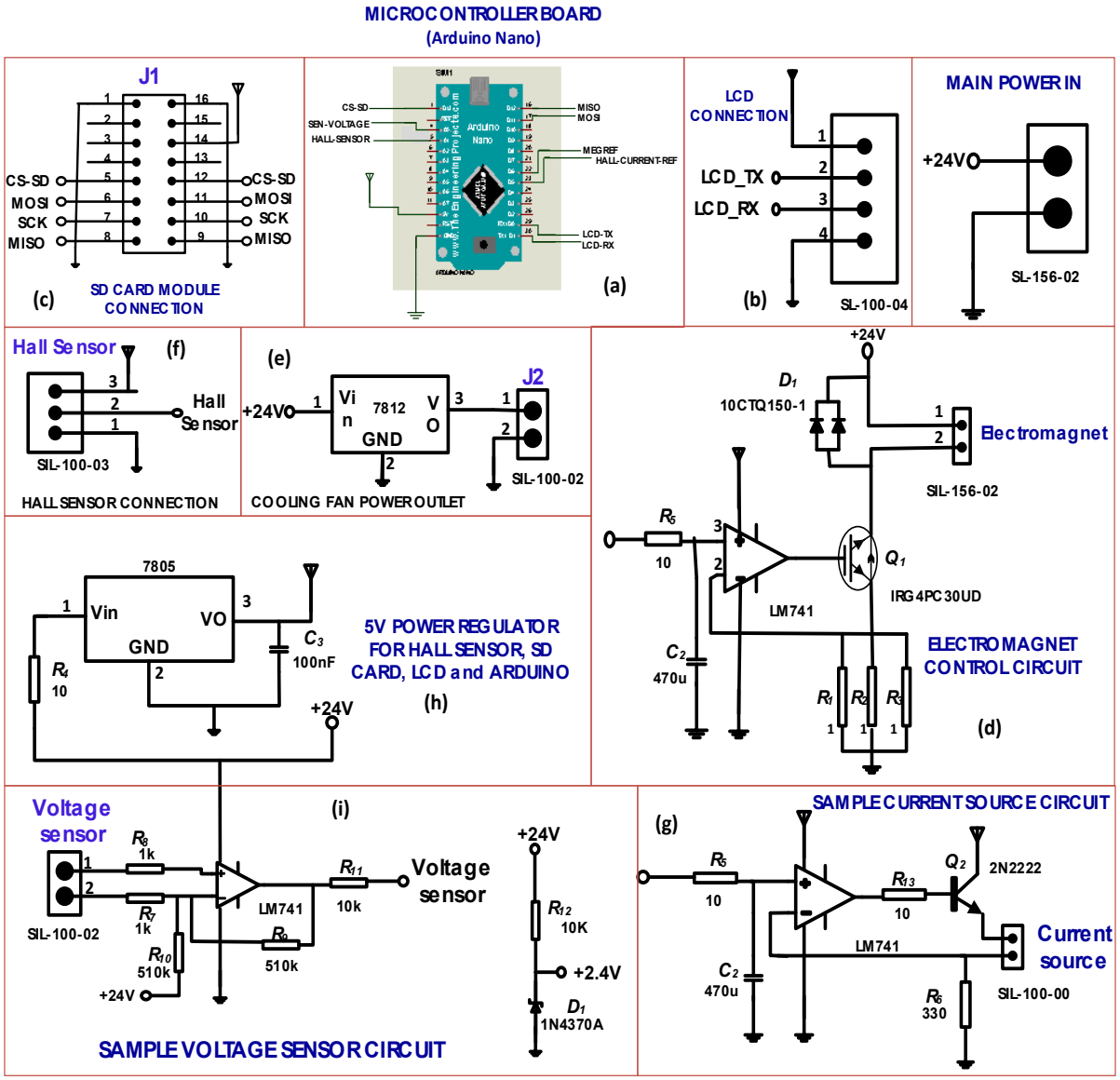

Figure 3: Circuit design board (a) microcontroller board (Arduino nano) (b) LCD connection, main power in (c) SD card module connection (d) electromagnet control circuit (e) cooling fan power outlet (f) hall sensor connection (g) sample current source circuit (h) 5V power regulator for hall sensor, SD card, LCD and Arduino (i) sample voltage sensor circuit.

5.3. Arduino Nano Microcontroller

Arduino Nano microcontroller is an electronic device. We may call it a minicomputer that cannot only store data but also process it. It is programmed in such a way that it deals with the hardware of our assembly. We can introduce Arduino as an open-source platform that is widely used in electronic projects. Arduino is all about a physical programmable circuit board, which is simply called a microcontroller, and a piece of software or IDE (Integrated Development Environment), that is used to run the computer code on the physical board.

5.4. Display Unit

The display unit is a Human Machine Interface to observe our measurement in digital form as well as to get the graphical representation; it is compatible with different programming languages like P_i·A+, P_i·B+, and Arduino. The display unit is shown in Figure 5. The Values of the magnetic field and sample current are mentioned in Figure 5; the red line is for V_H versus I, and the blue line is for V_H versus

Figure 4: A U-shaped soft iron-core electromagnet with pointing magnetic poles

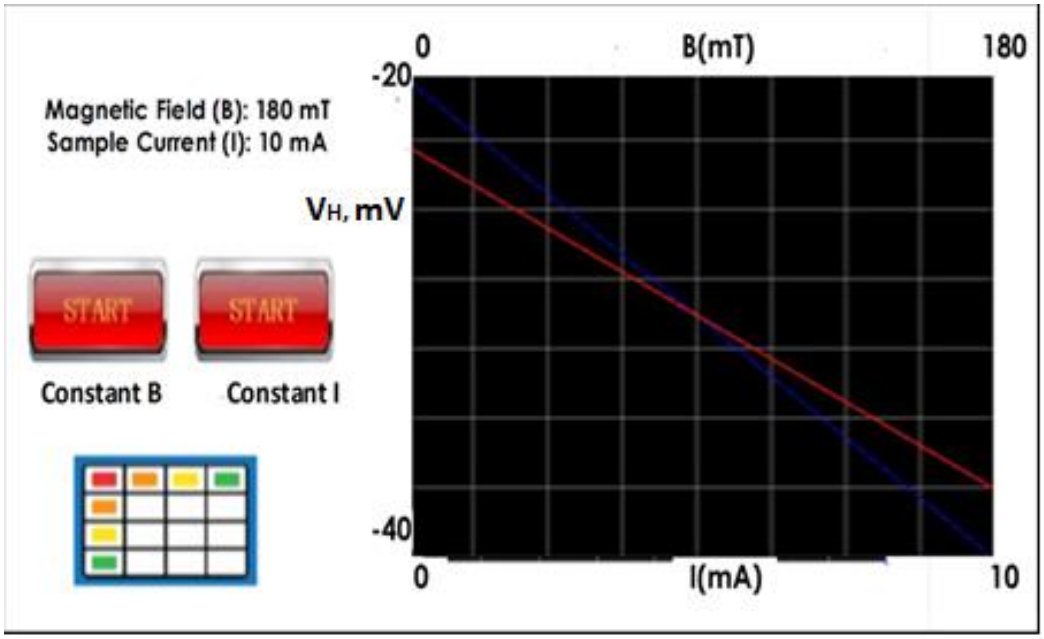

Figure 5: Display unit showing the screen of the Hall Effect device

magnetic field, B.

5.5. Sensors

Sensors are used to sense Hall Voltage, Hall current, and magnetic field under the principle of the Hall Effect. We can also measure the magnitude of the magnetic field of electromagnets used in a device through this. Its output voltage tells us about the strength of the magnetic field as it is directly proportional to the magnetic field strength. The Hall sensor used in a device is Honeywell SS495A, which operates on a supply voltage of 3 to 6.5 Volts. Its datasheet tells us that its sensitivity is 2.5mV/G. Its output voltage ranges from 0.86V to 4.21V and is very lightweight with a mass of only 0.11g. Its sensitivity impacts the accuracy of measurements by determining how effectively it can detect small changes in magnetic fields, with higher sensitivity leading to more precise and accurate readings.

5.6. Regulators

Regulators are used for modifying the magnetic fields while keeping the specimen's current constant, and also to change the current while keeping the magnetic field constant. The final assembly of the main printed circuit board, which is named the Apparatus Circuit Board, is shown in Figure 6.

From the schematic diagram shown above, we can see that there are different circuits designed on this PCB. These circuits include the electromagnet current control circuit, sample current source circuit, and sample voltage sensor circuit. A +5V power regulator for Hall Sensor, SD card, LCD, and Arduino, along with an SD card module connection port, Microcontroller board, and a cooling fan power outlet, are also installed on this PCB. We can also see a few connections in this diagram, which include LCD connections and Hall Sensor Connections [5-8].

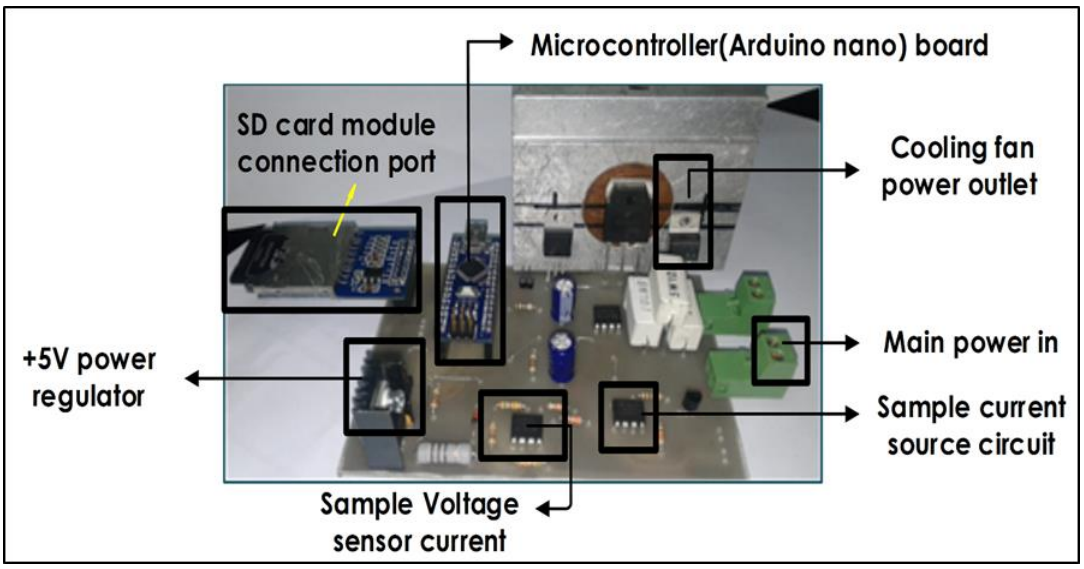

Figure 6: Final assembly of the device and main circuit board

5.7. Sample PCB

PCB was designed on the principle of the four-probe method. It is used to measure the electrical impedance using separate pairs of current-carrying and voltage-sensing terminals by making the measurements more accurate than the simple two-probe method. The four-probe method can be better understood from Figure 7 given below:

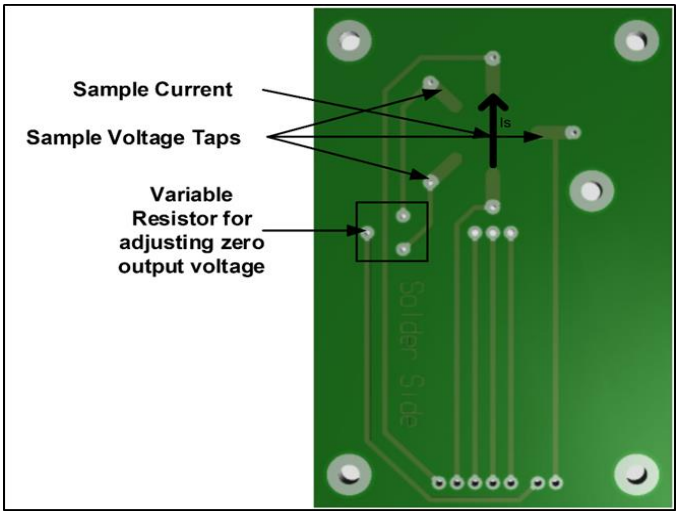

Figure 7: Sample printed circuit board

5.8. Heating Chamber and Temperature Control System

In the beginning, when the apparatus was being tested, the appropriate results were not being observed; in fact, the current was not passing through the semiconductor sample. The reason behind this was the fact that the semiconductors behave as an insulator at room temperature. To get the results, the temperature of the sample must be increased up to about 50 degrees centigrade. So, for this purpose, a heat chamber must be introduced to raise the temperature. The heating chamber that is installed in this apparatus can raise the temperature to 300˚C. So, along with this heating chamber, a temperature control system must also be introduced to avoid any catastrophe due to an increase in temperature. There is a temperature control system installed to avoid any damage, which shows the temperature of the system. By incorporating temperature sensors and heaters/coolers, we maintained a stable temperature, ensuring accurate Hall voltage readings despite temperature variations. The heating chamber of the device is shown in Figure 8.

Figure 8: Heating chamber with the heating element

In the final assembly, all the components of the project are combined to give a stand-alone system. The details of our final assembly are as follows:

Basically, three main chambers were made. One is for the electromagnet, another is for the heat source, and the last one is for the apparatus circuit board. This can be seen easily from the picture given below, i.e., Figure 9.

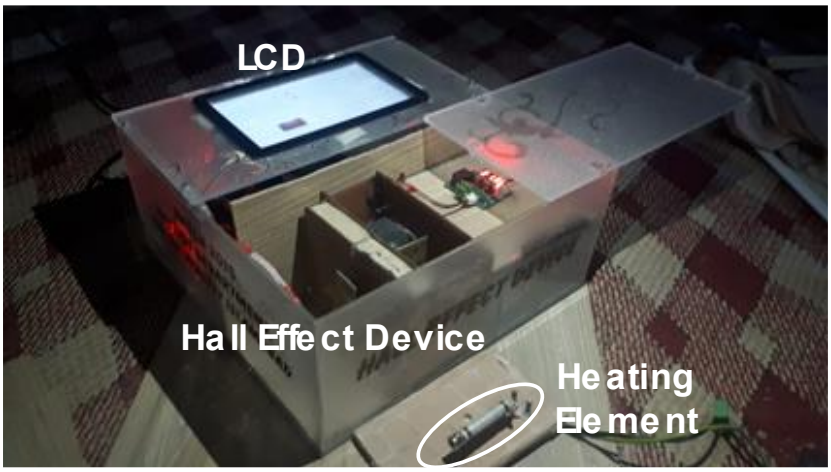

Figure 9: Hall Effect automated device for temperature control

6. Device Operation and Functioning

Our device hardware has four major components on a single board. These are electromagnets, the main circuit board, a sample circuit board, a temperature control system, and an LCD for display. This apparatus is a single-unit assembly having all inputs and outputs on a single board. A common power supply will give power to electromagnets, temperature control systems, voltage and current regulators, and the most important sample current.

The data after various measurements will be recorded and will take a presentable form through AVR microcontroller programming, and can be displayed through HMI.

Window display-1 is for selecting a constant magnetic field or a constant sample current. After selecting one of them, we will be able to get two graphs: one for constant magnetic field versus hall voltage and one for constant sample current versus hall voltage.

Window display-2 shows a table representing the variation of the hall voltage with respect to changing the magnetic field and changing the sample current separately. We can observe these variations of hall parameters at different temperatures as well with our temperature control system by placing the sample in a heating chamber and raising its temperature up to 300℃. Moreover, using electromagnetic shielding to block external noise and implementing low-pass filters to eliminate high-frequency noise. By using twisted pair cables, we reduce electromagnetic interference. Finally, proper grounding to avoid ground loops and using differential measurement techniques for noise cancellation.

7. Results and Discussion

Here we have tested some samples of semiconductor materials and then compared them with theoretically measured values of the Hall coefficient using formulas given in the introduction part, and as a result, we get the Hall coefficient values measured through our apparatus very close to the theoretical values [8, 9]. A graphical behavior of Hall voltage with respect to variations in the magnetic field and applied sample current is presented in the figure below.

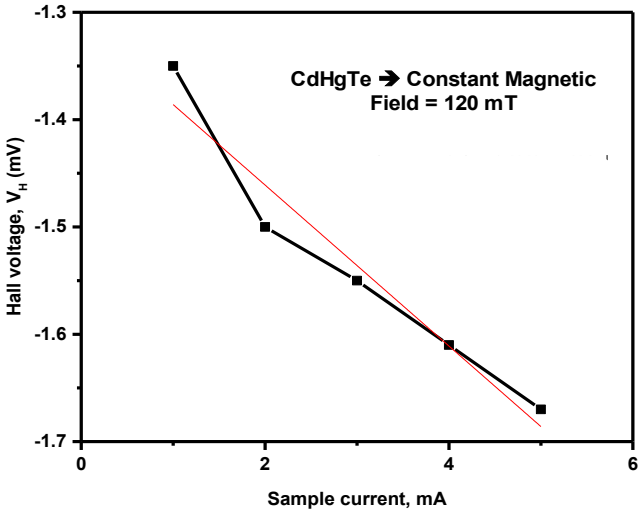

Equation	y = a + b*x		
Weight	No Weighting		
Residual Sum of Squares	0.00327		
Pearson's r	-0.97214		
Adj. R-Square	0.92675		
		Value	Standard Error
	Intercept	-1.311	0.03463
	Slope	-0.075	0.01044

Figure 10: Typical V_H versus sample current characteristics of CdHgTe with a constant magnetic field

Using the above plots, we can find the different Hall Effect parameters like carrier concentration, Hall coefficient, mobility, and resistivity of semiconductor materials in relation to $R_H = \frac{1}{ne}$ for the hall coefficient, while carrier concentration n can be determined using the relation $n = -\frac{I_x B_z}{tqV_H}$ for electrons and $p = \frac{I_x B_z}{tqV_H}$ for holes. This $\mu_n = \frac{I_x L}{wtqnV_x}$ relation is used to determine the electron mobility while $\mu_p =$

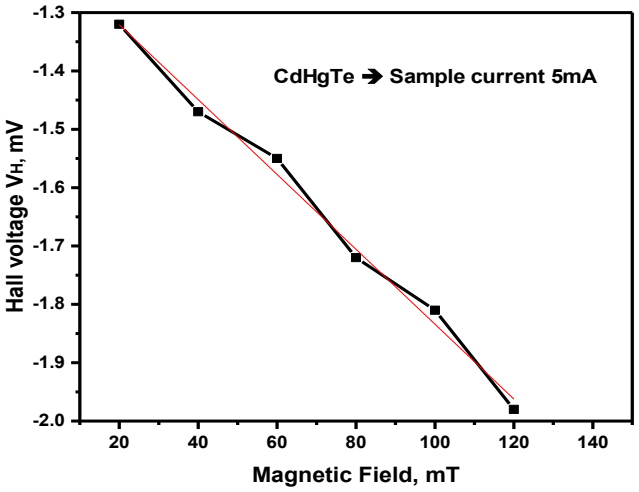

Equation	y = a + b*x		
Weight	No Weighting		
Residual Sum of Squares	0.00228		
Pearson's r	-0.99606		
Adj. R-Square	0.99017		
		Value	Standard Error
	Intercept	-1.19267	0.02224
	Slope	-0.00641	2.85476E-4

Figure 11: Typical V_H versus magnetic field characteristics of CdHgTe with constant sample current

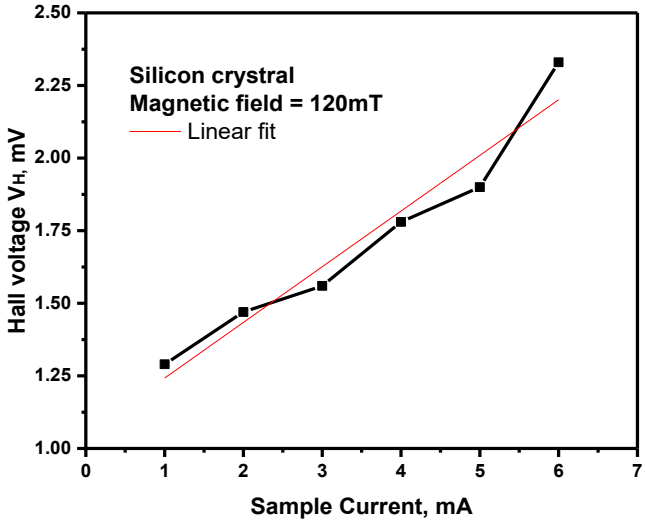

Equation	y = a + b*x		
Weight	No Weighting		
Residual Sum of Squares	0.03788		
Pearson's r	0.97179		
Adj. R-Square	0.93047		
		Value	Standard Error
	Intercept	1.05067	0.0906
	Slope	0.19171	0.02326

Figure 12: Typical V_H versus sample current characteristics of silicon with a constant magnetic field

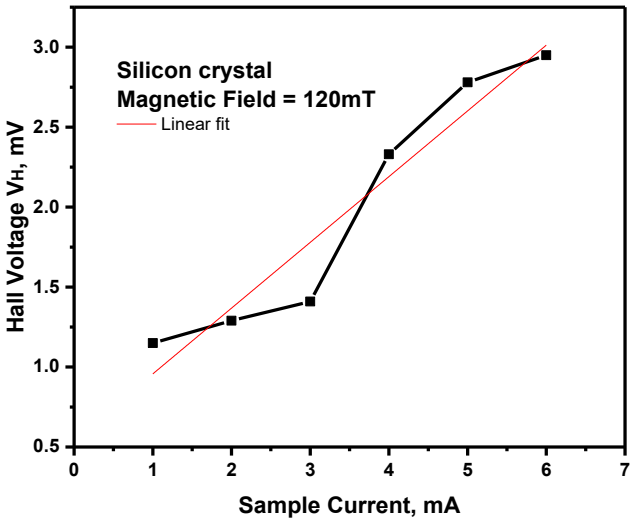

Equation	y = a + b*x		
Weight	No Weighting		
Residual Sum of Squares	0.23498		
Pearson's r	0.9625		
Adj. R-Square	0.90802		
		Value	Standard Error
?$OP.A=1	Intercept	0.546	0.22564
	Slope	0.41114	0.05794

Figure 13: Typical V_H versus sample current of Silicon crystal with constant magnetic field

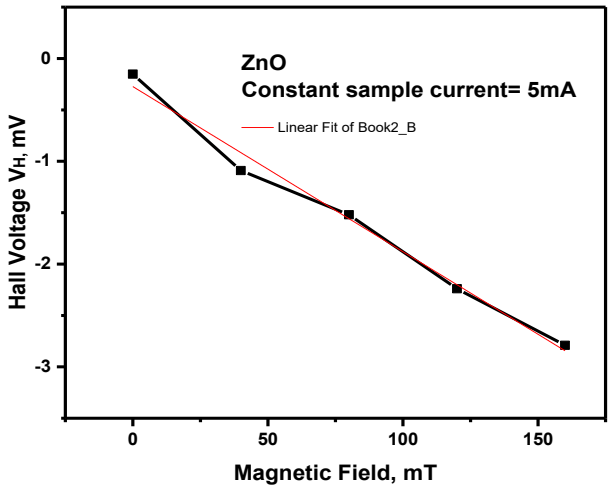

Equation	y = a + b*x		
Weight	No Weighting		
Residual Sum of Squares	0.0509		
Pearson's r	-0.99389		
Adj. R-Square	0.98376		
		Value	Standard Error
	Intercept	-0.2732	0.1009
	Slope	-0.01607	0.00103

Figure 14: Typical V_H versus magnetic field characteristics of ZnO with constant sample current.

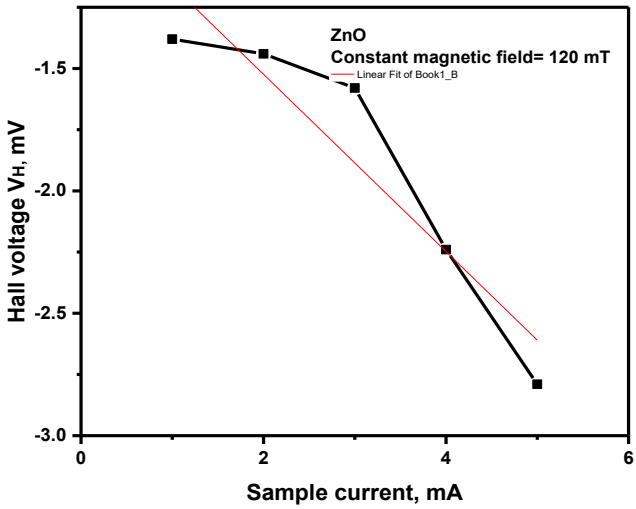

Equation	y = a + b*x		
Weight	No Weighting		
Residual Sum of Squares	0.18068		
Pearson's r	-0.93746		
Adj. R-Square	0.83844		
		Value	Standard Error
Book1_B	Intercept	-0.8	0.25739
	Slope	-0.362	0.07761

Figure 15: Typical V_H versus sample current characteristics of ZnO with a constant magnetic field

$\frac{I_X L}{wtqpV_X}$ for hole mobility. After getting suitable results of the Hall coefficient and mobility, the resistivity value can also be determined with the relation $\rho = \frac{R_H}{\mu}$. After getting slopes from the above plots and using the slopes in these relations, we can get these results whose values are comparable with the values mentioned in the literature [9], [10].

In Table 1, three samples were investigated through the Hall Effect automated device, and the obtained results were compared with other investigation techniques. The CdHgTe is one of the available semiconductor samples consisting of semimetals, and it provides an option to get the optimized bandgap; its Hall Effect parameters are mentioned in Table 1 [11], [12].

The second sample is ZnO, another semiconductor material representing all the parameters compared with the literature. The negative sign is due to the negative slope in the plots above, which also represents that we have n-type semiconductors [13], [14].

Silicon is another semiconductor material with comparable values of positive carrier concentration, Hall coefficient, mobility, and resistivity, with the literature showing this material is p-type [15], [16].

Table 1. A comparative table for Hall Effect parameters of different materials

Sample Name	Proposed Design HE Parameters				HE parameters in Literature [13] [14] [15] [16]			
	Carrier Con. (cm^{-3})	Hall Coef., R_H (cm^3C^{-1})	Mobility, ($cm^{-2}V^{-1}s^{-1}$)	Resistivity, Ω-cm	Carrier Con. (cm^{-3})	Hall Coef., R_H (cm^3C^{-1})	Mobility ($cm^{-2}V^{-1}s^{-1}$)	Resistivity, Ω-cm
Cadmium mercury telluride (CdHgTe)	-10×10^{20}	-6.2×10^{-3}	4.16	1.5×10^{-3}	10^{17}-10^{20}	10^{-2}-10^{-3}	1-100	~10^{-3}
n-type Zinc Oxide (ZnO)	-2×10^{18}	-3.12	44.2	2×10^{-3}	~10^{20}	10^{-1}-10^{-3}	~10	~10^{-3}
n-type Silicon p-type	7.5×10^{18}	0.83	219	3.8×10^{-3}	~10^{14}-10^{20}	~10^{-1}-10	10-10^2	~10^{-1}-10^{-3}

8. Conclusions and Future Direction

The development of an advanced Hall Effect Apparatus (HEA) utilizing modern technology and microcontrollers with a graphical user interface (GUI) have significantly improved the study of Hall Effect parameters in semiconductor materials. The new system demonstrates remarkable efficiency, providing 90% accuracy at a fraction of the cost of traditional methods. Experiments on semiconductor samples, including CdHgTe, ZnO, and silicon, confirmed the system's ability to accurately measure carrier concentrations, Hall coefficients, Hall mobility, and resistivity. These findings align closely with existing literature, validating the system's reliability.

Future work will focus on expanding the capabilities of the HEA by incorporating additional sensors and automated data analysis features to further enhance precision and user experience. Efforts will also be made to explore the application of this system in a wider range of semiconductor materials and to optimize the system for educational purposes, allowing students and researchers to gain hands-on experience with advanced data acquisition techniques. Additionally, integrating machine learning algorithms could provide predictive insights into semiconductor behavior under various conditions, offering a deeper understanding and new research opportunities in the field of condensed matter physics.

Acknowledgment

This research was supported by the Department of Physics, Air University, Islamabad; Department of Physics, Material Synthesis Lab, Fatima Jinnah Women University, Rawalpindi; Department of Research and Development, Tesla Industries, Islamabad, Pakistan.

Conflict of Interests

The authors declare no conflicts of interest regarding this article.

Funding Statement

This research article is not a product of a funded research project.

9. References

[1] A. C. Melissinos, *Experiments in Modern Physics*, Academic Press, 2003, pp. 63-71.

[2] S. O. Kasap, *Principles of Electronic Materials and Devices*, McGraw-Hill, 2006, pp. 145-148.

[3] Honeywell, *Hall Effect Sensing and Application*. [Online]. Available: http://sensing.honeywell.com. [Accessed: 9-Aug-2024].

[4] I. Simaciu, *Physics – Laboratory Guide*, Editura Universităţii Petrol-Gaze din Ploieşti, 2009.

[5] Z. Borsos, A. Baciu, M. Hotinceanu, I. Simaciu, L. Dumitraşcu, and G. Nan, "The Hall Effect Experiment Using New Data Acquisition and Processing Methods," *Bul. Univ. Petrol – Gaze din Ploieşti*, vol. LXII(2), pp. 28-35, 2010.

[6] C. Kittel, *Introduction to Solid State Physics*, John Wiley and Sons, 2005, pp. 216-226.

[7] S. O. Kasap, *Principles of Electronic Materials and Devices*, McGraw-Hill, 2006, pp. 145-148.

[8] A. Sconza and G. Torzo, "An undergraduate laboratory experiment for measuring the energy gap in semiconductors," *European Journal of Physics*, vol. 10(2), pp. 123, 1989.

[9] N. Moşescu, A. Baciu, and G. Nan, *Fizică*, Editura Universităţii Petrol-Gaze din Ploieşti, 2003.

[10] J. Thompson, P. Mackett, L. M. Smith, D. J. Cole-Hamilton, and D. V. Shenai-Khatkhate, "The growth of CdHgTe by MOCVD at reduced temperatures," *Journal of Crystal Growth*, vol. 86(1–4), pp. 233-239, 1988.

[11] J. C. Shim, Y. G. Kim, Y. T. Song, J. K. Hong, S. K. Hong, S. U. Kim, and M. J. Park, "The minority carrier mobility of HgCdTe measured by the modulated Hall Effect," *Journal of Crystal Growth*, vol. 214–215, pp. 260-264, 2000.

[12] G. Korotaev, I. I. Izhnin, K. D. Mynbaev, A. V. Voitsekhovskii, S. N. Nesmelov, S. M. Dzyadukh, O. I. Fitsych, V. S. Varavin, S. A. Dvoretsky, N. N. Mikhailov, M. V. Yakushev, O. Y. Bonchyk, H. V. Savytskyy, Z. Swiatek, and J. Morgiel, "Hall-effect studies of modification of HgCdTe surface properties with ion implantation and thermal annealing," *Surface and Coatings Technology*, vol. 393, pp. 125721, 2020.

[13] N. Jahed and S. Sivoththaman, "Systematic control of carrier concentration and resistivity in RF sputtered Zinc oxide thin films," *arXiv*, 2014. [Online]. Available: https://arxiv.org/abs/1404.4902. [Accessed: 9-Aug-2024].

[14] F. Schindler, J. Geilker, W. Kwapil, W. Warta, and M. C. Schubert, "Hall mobility in multicrystalline silicon," *Journal of Applied Physics*, vol. 110(4), p. 043722, 2011.

[15] R. Akram, "Effects of Temperature, Thickness and Bias Current on Magnetoelectric Characteristics of Silicon Micro-Hall Sensors," *Arabian Journal for Science and Engineering*, vol. 44, pp. 541–552, 2019.

[16] R. Akram, "Application of silicon micro hall sensors in variable temperature scanning hall probe microscopy (SHPM) using multiple feedback techniques," *International Journal of Advanced and Applied Sciences*, vol. 5(6), pp. 70-78, 2018.